
Smooth approximations of single-input optimal orbital transfer using continuation and averaging techniques

Bernard BONNARD* — **Jean-Baptiste CAILLAU**** — **Romain DUJOL****

** Institut de Mathématiques de Bourgogne
F-21078 Dijon, FRANCE*

*** ENSEEIHT-IRIT
F-31071 Toulouse, FRANCE*

ABSTRACT. This article deals with the optimal transfer of a satellite between Keplerian orbits when the control is oriented along the tangential direction. We consider the time-optimal control problem and the energy minimization problem. The optimal controls laws have discontinuities and continuations and averaging techniques are applied to smooth the discontinuities. The smooth approximations of the solutions are computed using a shooting method taking into account second-order optimality conditions.

RÉSUMÉ.

KEYWORDS: Optimal control, shooting method, second-order optimality condition, single-input orbit transfer, continuation method, averaging

MOTS-CLÉS :

1. Introduction

The orbital transfer is described by the *controlled KEPLER equation*

$$\ddot{q}(t) = -\mu \frac{q(t)}{|q(t)|^3} + \frac{u(t)}{m(t)}, \quad (1)$$

and the mass variation equation

$$\dot{m}(t) = -\beta |u(t)| \quad (2)$$

where the gravitation constant μ is normalized to 1, $q \in \mathbf{R}^3$ is the position of the satellite in a fixed frame whose origin is the Earth center, m is the mass, $\beta > 0$ and $u \in \mathbf{R}^3$ represents the thrust, satisfying $|u| \leq \varepsilon$, and the maximal thrust is small for *low propulsion*.

Two relevant optimal control problems are the *time-optimal* control problem (the transfer time can take several months) and the *energy minimization problem* : $\text{Min}_{u(\cdot)} \int_0^T |u|^2 dt$, this second problem is a regularization of the minimum-fuel optimal problem, which amounts to an L^1 -minimization problem, see [Ger ar].

The thrust can be decomposed in the *tangential-normal frame*

$$u = u_t F_t + u_n F_n + u_c F_c \quad (3)$$

where F_t, F_n, F_c form an orthonomous frame and F_t is colinear to $\partial/\partial \dot{q}$, F_c is perpendicular to the osculating plane $\text{Span}\{q, \dot{q}\}$, and $F_n = F_c \wedge F_t$.

An important subproblem is to consider the case where the control is oriented along the tangential direction F_t alone, and the system becomes single-input. This, in order to understand the effect of each control component u_t, u_n or u_c . Moreover, in electro-ionic propulsion, due to technologic reasons, we must impose *cone constraints* on the control directions.

Due to this restriction, the optimal solutions are not smooth. A consequence is a numerical instability in shooting methods. Moreover, the second-order conditions implemented in the COTCOT code [BON 06e] require smooth extremals. The objective of this article is to present smooth approximations using continuations and homotopic techniques, which allow to handle numerically the optimal problems, using a shooting method, taking into account second-order optimality conditions.

2. The time-minimal control problem

2.1. Preliminaries

The controlled KEPLER equation where the control is decomposed in the tangential-normal frame is written

$$\dot{x}(t) = F_0(x(t)) + \frac{1}{m(t)} \sum_{i=1}^3 u_i(t) F_i(x(t)) \quad (4)$$

where $|u| \leq \varepsilon$. According to [Cai 00] the time-optimal transfer is almost everywhere with maximal thrust $|u| = \varepsilon$ and $m(t)$ can be computed integrating (2). Moreover, excepted isolated singularities that can be handled numerically, an optimal control is *smooth* and is given by

$$u = \frac{\varepsilon(H_1, H_2, H_3)}{|(H_1, H_2, H_3)|} \quad (5)$$

where H_i is the Hamiltonian lift $\langle p, F_i \rangle$ and p is the adjoint vector, solution of the adjoint system.

If we consider the single-input case, where u_t is oriented along F_t , the system takes the form

$$\dot{x}(t) = F_0(x(t)) + \frac{u_t(t)}{m(t)} F_t(x(t)) \quad , \quad |u_t| \leq \varepsilon ,$$

and for geometric analysis we can assume that the mass is constant. Since the thrust is oriented along the osculating plane, the state $x = (q, \dot{q})$ is restricted to the four-dimensional space formed by its tangent space. Hence, we can only transfer the system towards a *coplanar* orbit. We introduce the so-called *elliptic domain* filled by the elliptic orbits of KEPLER equation,

$$X = \{(q, \dot{q}) \mid q \wedge \dot{q} \neq 0, H(q, \dot{q}) < 0\}$$

where $H(q, \dot{q}) = |\dot{q}|^2/2 - 1/|q|$ is the energy of the KEPLER equation.

Using the analysis of [BON 05c] we have

Proposition 2.1.

- (i) *The system restricted to the elliptic domain is controllable.*
- (ii) *Every time-optimal control is bang-bang, i.e. $u^*(t) = \varepsilon \operatorname{sign}\langle p, F_t(x) \rangle$, where p is the adjoint vector, and with a finite number of switchings.*

2.2. The shooting method

We briefly recall the shooting method applied to the time-minimum problem, with fixed extremities x_0 and x_f . We consider a system of the form

$$\frac{dx}{dt}(t) = f(x(t), u(t)) \quad , \quad (x, u) \in X \times U ,$$

where X is a n -dimensional manifold and U is the control domain. The *pseudo-Hamiltonian* associated with the time-optimal control problem is

$$H(x, p, u) = \langle p, f(x, u) \rangle.$$

From PONTRYAGIN's maximum principle every optimal trajectory is a projection of a *BC-extremal* (z, u) , $z = (x, p)$ solution of the boundary value problem

$$\begin{aligned} \dot{x} &= \frac{\partial H}{\partial p}(x, p, u), \\ \dot{p} &= -\frac{\partial H}{\partial x}(x, p, u), \\ x(0) &= x_0, x(t_f) = x_f \end{aligned} \tag{6}$$

where u is computed using the maximization condition

$$H(x, p, u) = \text{Max}_{v \in U} H(x, p, v). \tag{7}$$

By homogeneity, the adjoint vector can be restricted to the projective space $\mathbf{P}(T_x^*X)$ and the maximum of (7) is constant along a reference extremal. We introduce the shooting mapping.

Definition 2.1. We fix x_0 and we consider all the extremal curves $z(t) = (x(t), p(t))$ starting at time 0 from x_0 and depending upon $p(0) = p_0$. The shooting mapping is $S : (p_0, t_f) \mapsto x(t_f, p_0) - x_f$, where u is computed using the maximization condition. Solving the boundary value problem reduces to solve the shooting equation $S(p_0, t_f) = 0$.

2.3. JACOBI equation. Conjugate point

2.3.1. Main assumption

We assume that the control domain is an m -dimensional manifold and restricting to a chart, the maximization condition implies

$$\frac{\partial H}{\partial u} = 0. \tag{8}$$

We consider a reference extremal $z(t) = (x(t), p(t))$ defined on $[0, T]$ and we assume the *strict LEGENDRE condition* along $z(t) : \partial^2 H / \partial u^2 < 0$ so that the control can be computed as a *smooth* mapping $u_r(z)$. Plugging u_r into $H(z, u)$, we define a *true smooth Hamiltonian* $H_r(z)$.

For a fixed x_0 , let $z(t, p_0)$ be the extremal solution of $\overrightarrow{H_r}$ with initial condition $p_0 \in \mathbf{P}(T_{x_0}^*X)$. If Π is the projection $(x, p) \mapsto x$, the *exponential mapping* is

$$\exp_{x_0} : (t, p_0) \mapsto \Pi(z(t, p_0)) = x(t, p_0).$$

For a fixed t , the image is the projection of the $(n-1)$ -manifold $L(t) = \{z(t), p_0 \in \mathbf{P}(T_{x_0}^*X)\}$, and the previous shooting mapping is $S(p_0, t_f) = \exp_{x_0}(t_f, p_0) - x_f$.

Definition 2.2. Let $z(t) = (x(t), p(t))$, $t \in [0, T]$, be the reference extremal. The JACOBI equation is the variational equation $\dot{\delta z}(t) = d\vec{H}_r(z(t)) \delta z(t)$. The non-trivial solutions of this equation are called JACOBI fields. Let $J(t) = (\delta x(t), \delta p(t))$ be a JACOBI field, J is said vertical at time t if $\delta x(t) = 0$. A time $t_c > 0$ is said to be conjugate if there exists a JACOBI field vertical at time $t = 0$ and $t = t_c$. The point $x(t_c)$ is then called a conjugate point.

A straightforward result is the following.

Proposition 2.2. A time t_c is conjugate if and only if the derivative of the exponential mapping with respect to p_0 is not of full rank at $t = t_c$.

2.4. Second-order sufficient condition

We make the following additional assumptions. The reference extremal trajectory $t \mapsto x(t)$ is one-to-one on $[0, T]$. Moreover we assume that on each subinterval $0 \leq t_0 < t_1 \leq T$ the adjoint vector p is unique up to a scalar and we are in the so-called *normal case* where $H = \langle p, f(x, u) \rangle$ is not zero. Hence p can be normalized, for instance by being chosen on the level set $\langle p, f(x, u) \rangle = 1$. We have the following [SAR 82].

Proposition 2.3. The reference extremal $t \mapsto x(t)$ is optimal in the C^1 -topology up to the first conjugate time t_{1c} and no more optimal if $t > t_{1c}$.

To get C^0 -optimality we proceed as follows. If there exists no conjugate point on $[0, T]$, we can embed the reference trajectory into a *central field* \mathcal{F} formed by all extremal curves at time t of all extremal curves starting from x_0 . At time t , this field is the projection of $L(t)$. This construction is valid in a neighbourhood of the reference curve, but it can be prolonged to a maximal open set W homeomorphic to a convex cone. The important result is the following [BON 05a].

Proposition 2.4. Excluding x_0 , assume that there exists an open neighbourhood W of the reference trajectory in the C^0 -topology and two smooth mappings $V : W \rightarrow \mathbf{R}$ and $\hat{u} : W \rightarrow U$ such that for each (x, u) in $W \times U$, we have the maximization condition

$$H(x, dV(x), \hat{u}(x)) \geq H(x, dV(x), u).$$

Then the reference trajectory is optimal among the trajectories of the system with the same extremities and contained in W .

Remark 1. The construction of V is equivalent to solve the standard HAMILTON-JACOBI-BELLMAN equation

$$\max_{u \in U} H \left(x, \frac{\partial V}{\partial x}(x), u \right) = 1,$$

and the transfer time between x'_0 and x'_1 in W is $V(x'_1) - V(x'_0)$, the adjoint vector p being $\partial V / \partial x$.

The following is clear.

Proposition 2.5. *The shooting mapping S is a local diffeomorphism onto W .*

And the final result is

Theorem 2.6. *Under our assumptions, the reference curve is C^0 -optimal with respect to all curves solution of the system with same extremities and contained in the domain covered by the central field.*

The crucial computational point is to evaluate conjugate points and we have the following algorithm [BON 06e].

2.4.1. Computation of conjugate points

Let $(J_i)_i$ with $J_i(0) = (0, \delta p_i(0))$, $i = 1, \dots, n-1$ be a basis of JACOBI fields that are vertical at time $t = 0$, $\delta p(0)$ being normalized by $p(0)\delta p(0) = 0$. The time t_c is conjugate if and only if the rank of the matrix $C(t)$ whose columns are $\delta x_j(t)$, $1 \leq j \leq n-1$ is strictly less than $n-1$ at $t = t_c$.

The numerical efficient test about the rank is provided by a *singular value decomposition* (SVD) of the matrix $C(t)$. If $\sigma_{n-1}(t)$ is the smallest singular value, the test is $\sigma_{n-1}(t_c) = 0$.

This theory requires the Hamiltonian to be smooth, so it cannot be applied to analyze the single-input orbital transfer and we shall need to smooth the Hamiltonian using regularizing processes such as those described in next section.

3. Continuation methods

Consider the time optimal control problem with fixed extremities x_0 and x_f and the shooting equation $S(p_0, t_f) = 0$. An important problem to ensure convergence is to have a *good initial guess* on p_0 . For this purpose a powerful method is the *continuation method* [All 90]. We embed the single-input transfer problem denoted (P_1) into a one-parameter family (P_λ) of problems where $\lambda \in [0, 1]$ with associated shooting equations $S_\lambda(p_0, t_f) = 0$. It was used in time optimal transfer by [Cai 00] (continuation on the maximal thrust ε) and in [Ger ar] (continuation between the energy minimization problem and the maximization of the final mass). A crucial property in such continuation methods is the regularity of the continuation path.

Next, we present two continuations to understand the single-input transfer and discuss the crucial smoothness property.

3.1. Continuation on the control domain.

We consider (P_0) as the transfer towards a coplanar orbit by setting $u_c = 0$, *i.e.* $u = u_t F_t + u_n F_n$ (see the decomposition in (3)) and connect the single-input transfer to a problem with two control entries.

The only difference between (P_0) and (P_1) is the set of admissible controls : for (P_0) , U_0 is the disc of centre $0_{\mathbf{R}^2}$ and radius ε , whereas for (P_1) , U_1 is the segment line $[-\varepsilon, \varepsilon]$ directed along the tangential direction (see fig. 1).

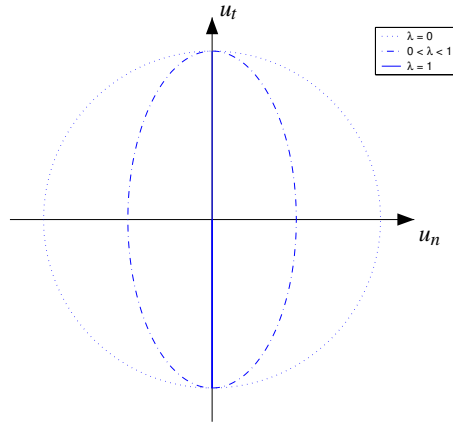


Figure 1. Continuation on the control domain

The homotopy can therefore be defined as follows. The problem (P_λ) is the orbital transfer with control domain U_λ where U_λ is the ellipse of centre $0_{\mathbf{R}^2}$, semi-major axis ε along the tangential direction, and semi-minor axis $(1 - \lambda)\varepsilon$ along the normal direction. Except at isolated singularities [Cai 00], the problem (P_λ) is smooth for λ in $[0, 1[$, and associated with the true Hamiltonian function

$$H_{r,\lambda}(t, x, p) = H_0 + \frac{\varepsilon}{m(t)} [H_1^2 + (1 - \lambda)H_2^2]^{1/2} \quad (9)$$

with, as before, $H_i = \langle p, F_i \rangle$, $i = 0, \dots, 3$, and $H_{r,\lambda} \rightarrow H_r = H_0 + (\varepsilon/m)|H_1|$ when $\lambda \rightarrow 1$.

3.2. Continuation on the inclination

We impose that the initial orbit, in contrast with the final one, does not belong to the equatorial plane, and we make a convex homotopy on the initial inclination (that is on the initial condition, see fig. 2) defined by the vector h of the equinoctial elements (see section 3.4):

$$h_{x,\lambda}(0) = (1 - \lambda)\eta \quad (10)$$

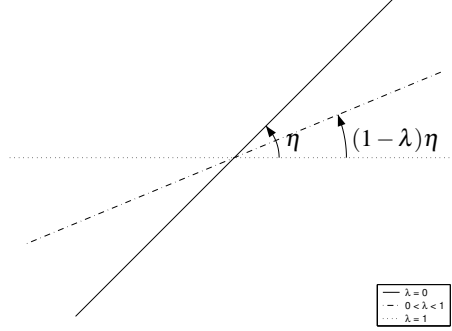


Figure 2. Continuation on the inclination

where $\eta \neq 0$ is the given initial inclination for the problem (P_0) . Indeed, the single-input transfer is a coplanar transfer and we use the following result [Cai 00].

Lemma 3.1. *Every extremal trajectory for the coplanar orbit transfer problem is also extremal for the general orbit transfer problem, provided the initial and final inclinations are the same.*

We define (P_0) by setting $u_n = 0$, i.e. $u = u_t F_t + u_c F_c$, and connect the single-input transfer to a problem with two controls, including a non-coplanar thrust u_c in this case.

3.3. Smoothness of the continuation path

According to our preliminary results in Section 2, we have the following (under assumptions therein).

Proposition 3.2. *Provided there is no conjugate point along the path, the mapping $\lambda \mapsto (p_0(\lambda), t_f(\lambda))$ associated with either of the two continuations is smooth for $0 \leq \lambda < 1$.*

Proof. Consider for fixed λ the shooting equation $S_\lambda(t_f, p_0) = 0$. If there is no conjugate point S_λ is of maximum rank and the equation can be smoothly solved using the implicit function theorem. \square

3.4. Numerical computations

For numerical reasons, we choose *equinoctial coordinates* [Cai 00] $(P, e_x, e_y, h_x, h_y, l)$ where P is the semi-latus rectum, $e = (e_x, e_y)$ the eccentricity vector, $h = (h_x, h_y)$ the inclination vector and l the longitude. The first five coordinates are *slow variables* corresponding to the first integrals of the uncontrolled motion, while l

is the *fast variable*. For the numerical computations, we consider the physicals values of tables 1 and 2, and we assume the mass is varying with equation 2.

Variable	Value	
ε	6	Newtons
μ	5165.8620912	$\text{Mm}^3.\text{h}^{-2}$
$\beta = V_e^{-1}$	0.0142	$\text{Mm}^{-1}.\text{h}$

Table 1. *Physical values*

Initial conditions			Final conditions	
P	11.625	Mm	42.165	Mm
e_x	0.75		0	
e_y	0		0	
h_x	$\eta = 0.0612$	rad	0	rad
h_y	0	rad	0	rad
l	π	rad	62.000	rad
m	1500	kg		

Table 2. *Boundary conditions*

3.4.1. Evolution of the optimal control along homotopies

We present in figures 3 and 4 the evolution of the optimal thrust along the homotopy path respectively for the homotopy on the control domain and the homotopy on the inclination.

We can see that switchings can be localized at the very beginning of the homotopy path, that for λ near 0. The remaining part of the homotopy path confirms this localization and tends to give the final shape of the optimal control. This phenomenon has already been observed in [Ger ar] for the minimum consumption problem where the homotopy consists in deforming an L^2 -cost into an L^1 -cost.

As a first comparison, we can also remark that the localization is far more efficient in the case of the homotopy on the inclination.

3.4.2. Computation of conjugate times

We can apply the conjugate point test on the intermediate problems (P_λ) for λ in $[0, 1[$, since they provide smooth extremals.

Once we have obtained an extremal by the shooting method, we extend this extremal up to several times the minimum time. Then we apply our test for fixed extremities to the extended extremal.

We present in the figures 5 and 6 the evolution of the smallest singular value along the homotopy path respectively for the homotopy on the control domain and the homotopy on the inclination. For λ near to 1, the first conjugate times found for both homotopies appear to be roughly the same.

We can notice that we have conjugate times at roughly three times the final time obtained by the shooting method, which confirms previous results [BON 05c].

3.4.3. Analysis of the extremal trajectories

We observe that zones where $u = \varepsilon$ (acceleration phases) are located around the apocenter. The apocenter is indeed the point where the gravitation is the weakest therefore it is the place where the acceleration is the most efficient. Conversely, zones where $u = -\varepsilon$ (deceleration phases) are located around the pericenter where the deceleration is the most efficient since the gravitation is the strongest at this point.

Finally, a preliminary interesting constatation on single-input transfers is that, compared to coplanar transfers with two thrusters, the minimum time is only increased of approximatively 20%. As illustrated by the second homotopy, a similar approach with two thrusters instead of three can be considered for non-coplanar transfers.

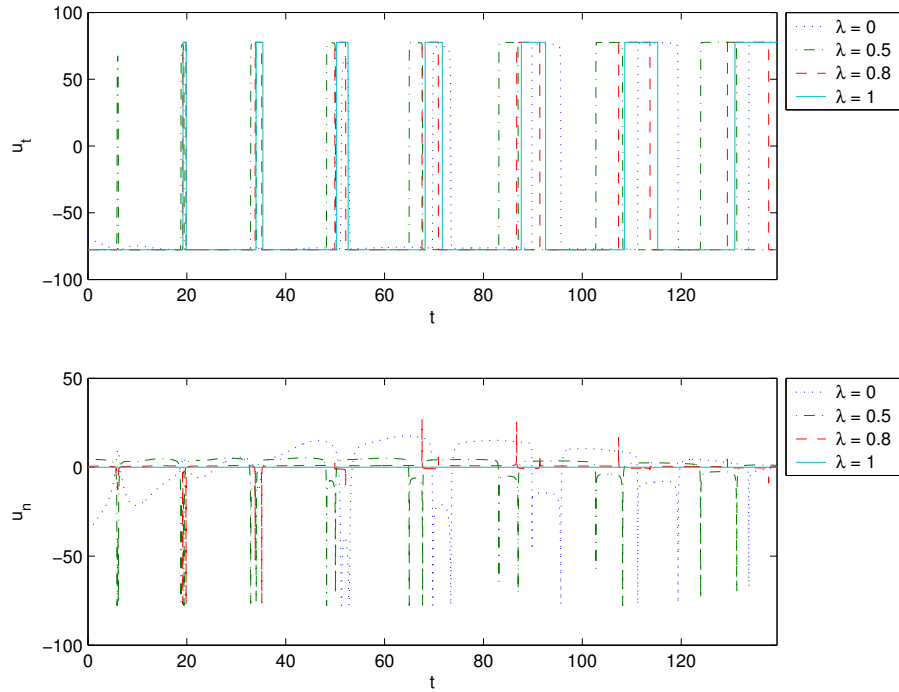


Figure 3. Optimal control: Homotopy on the control domain

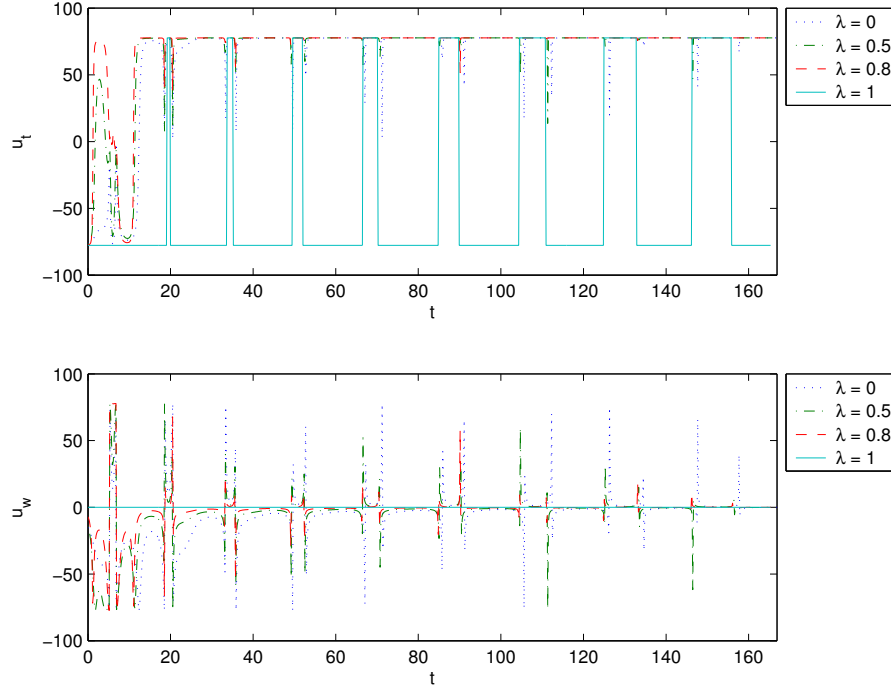


Figure 4. Optimal control: Homotopy on the inclination

4. Averaging method

4.1. Preliminaries

This method can be applied to every optimal transfer with low propulsion but an appropriate cost is the energy $c = \int_0^T u^2 dt$, where the transfer time is fixed. It leads to an averaged system which can be explicitly computed and has moreover a nice geometric interpretation. The control is rescaled by setting $u = \varepsilon u$, $|u| \leq 1$, as well as the cost ($c \rightarrow \varepsilon c$). To make the computation explicit, we drop the bound $|u| \leq 1$ and practically the constraint $|u| \leq 1$ will be fulfilled for large enough transfer times.

It is crucial to represent the system in the adapted coordinates of [GEF 97] denoted (v, x) where $x = (n, e, \omega)$ belongs to the *elliptic domain*,

$$X = \{n > 0, -1 < e < 1, \omega \in \mathbf{S}^1\}.$$

Herebefore, we have used the *elliptic elements* where n is the *mean movement* equal to $\sqrt{1/a^3}$ – a being the semi-major axis –, e is the *eccentricity*, ω is the *argument of*

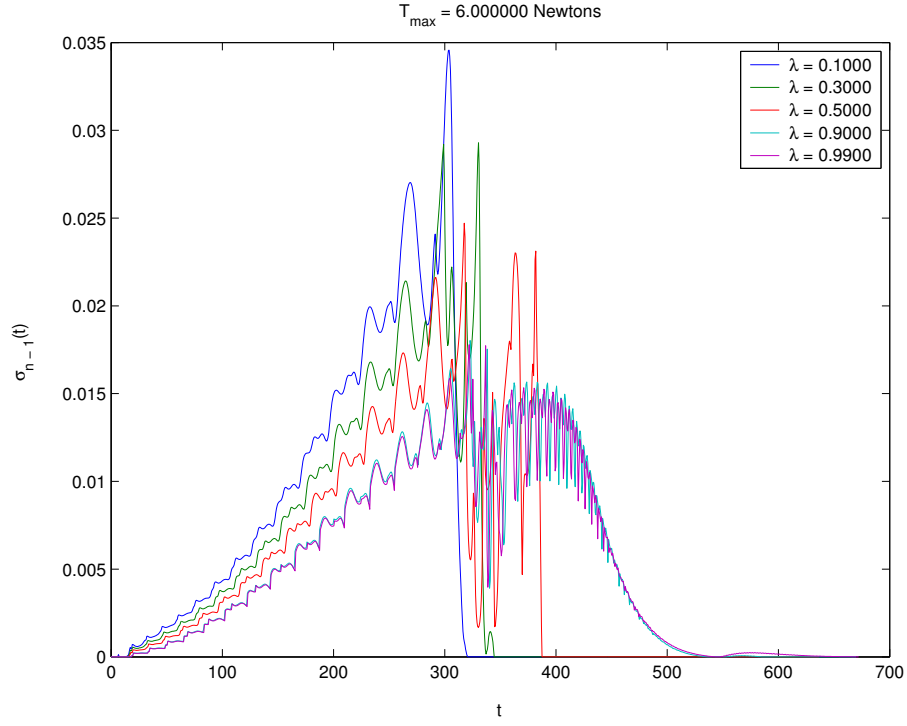


Figure 5. *Smallest singular value: Homotopy on the control domain*

the pericenter, and v is the true longitude corresponding to the angle of the pericenter: $v = l - \omega$ where l is the polar angle or longitude. The equations are:

$$\dot{n} = -3n^{2/3} \left(\frac{1 + 2e \cos v + e^2}{1 - e^2} \right)^{1/2} u, \quad (11)$$

$$\dot{e} = \frac{2(e + \cos v)}{n^{1/3}} \left(\frac{1 - e^2}{1 + 2e \cos v + e^2} \right)^{1/2} u, \quad (12)$$

$$\dot{\omega} = \frac{2 \sin v}{n^{1/3} e} \left(\frac{1 - e^2}{1 + 2e \cos v + e^2} \right)^{1/2} u, \quad (13)$$

$$\dot{l} = n \frac{(1 + e \cos v)^2}{(1 - e^2)^{3/2}}. \quad (14)$$

The coordinates are singular for circular orbits but the singularity $e = 0$ is removed by using the eccentricity vector

$$e_x = e \cos \omega, e_y = e \sin \omega.$$

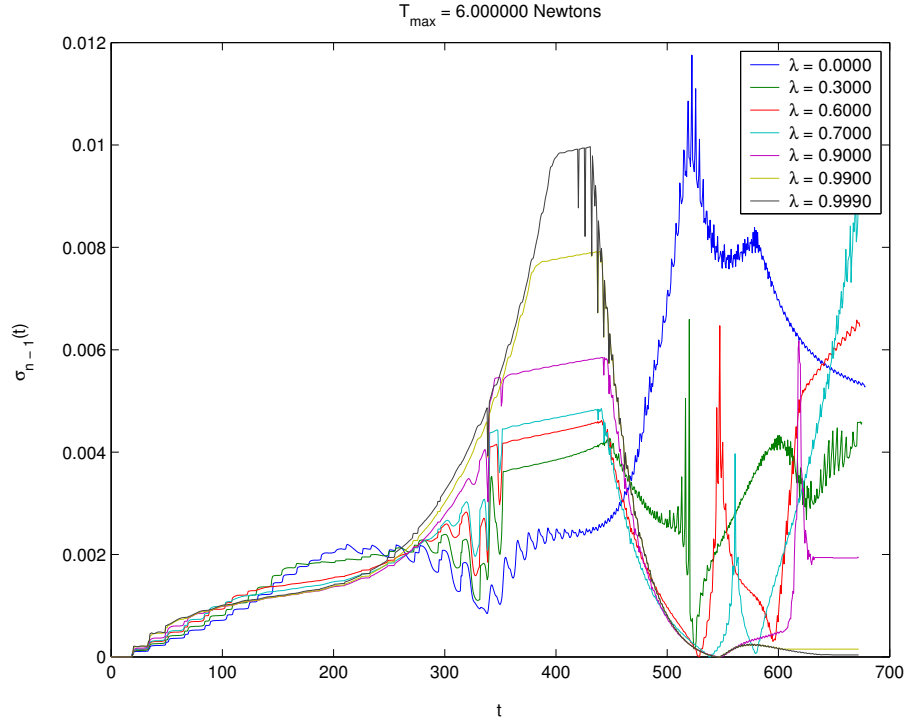


Figure 6. *Smallest singular value: Homotopy on the inclination*

The control system is of the form

$$\begin{aligned} \dot{l} &= \omega_0(l, x), \\ \dot{x} &= uF(l, x) \end{aligned}$$

where x is in X , l is in \mathbf{S}^1 , F is a smooth vector field on $\mathbf{S}^1 \times X$ and ω_0 is a smooth positive function defined on $\mathbf{S}^1 \times X$.

4.2. Minimum energy control and averaging

The energy can be written

$$\int_0^T u^2 dt = \int_{l_0}^{l_f} \frac{u^2 dl}{\omega_0(l, x)}$$

so that, after replacing time by cumulated longitude l , the Hamiltonian to consider from the maximum principle is

$$H(l, x, p, u) = \frac{p^0 u^2 + uP(l, x, p)}{\omega_0(l, x)},$$

and P is the Hamiltonian lift $\langle p, F(l, x) \rangle$.

Hence we have

$$H(l, x, p, u) = \varepsilon \frac{-u^2/2 + uP(l, x, p)}{\omega_0(l, x)}$$

where p^0 has been normalized to $-1/2$ in the *normal case* ($p^0 \neq 0$).

The maximization condition leads then to $\partial H / \partial u = 0$ and extremal controls are $u = P(l, x, p)$. Plugging such controls into H , we obtain the *true Hamiltonian*

$$H_r(l, x, p) = \varepsilon \frac{P^2(l, x, p)}{2\omega_0(l, x)}. \quad (15)$$

We drop the parameter ε , which amounts to parameterizing by $\tilde{l} = \varepsilon l$ instead of l . Since H is 2π -periodic in the angular variable, we introduce

Definition 4.1. *The averaged Hamiltonian is*

$$\bar{H}_r(x, p) = \frac{1}{2\pi} \int_0^{2\pi} H_r(l, x, p) dl.$$

From standard approximation results between trajectories of H_r and \bar{H}_r , the following is true [ARN 78].

Proposition 4.1. *Let $z(l)$ and $\bar{z}(l)$ be respective integral curves of H_r and \bar{H}_r with same initial conditions, then the difference $z - \bar{z}$ is uniformly of order $o(\varepsilon)$ for a length of order $1/\varepsilon$, and the difference between the respective energy costs is of order $o(\varepsilon^2)$.*

An important conceptual step introduced in [BON 05b] is to relate \bar{H} to an optimal control problem. We refer the reader to the sub-Riemannian formalism, see [BON 03] for details.

4.3. Averaged Hamiltonian of energy minimization coplanar transfer

4.3.1. Computations

According to equations (11)-(14), the true Hamiltonian $H_r(l, x, p)$ can be written $(1/2)\langle A(v, x)p, p \rangle$ where $A(v, x)$ is a symmetric matrix, see [BON 06c]. The averaged Hamiltonian is similarly written $(1/2)\langle \bar{A}(x)p, p \rangle$ where $\bar{A}(x)$ is the symmetric matrix whose elements are the averaged of the six coefficients of $A(v, x)$.

Proposition 4.2. *The matrix $\bar{A}(x)$ is diagonal and the averaged Hamiltonian is*

$$\bar{H}_r = \frac{1}{2n^{5/3}} \left[9n^2 p_n^2 + \frac{4(1-e^2)^{3/2}}{1+\sqrt{1-e^2}} p_e^2 + \frac{4(1-e^2)}{1+\sqrt{1-e^2}} \frac{p_\omega^2}{e^2} \right].$$

Theorem 4.3. *The averaged Hamiltonian \bar{H}_r is associated with the three-dimensional metric*

$$\bar{g} = \frac{dn^2}{9n^{1/3}} + n^{5/3} \frac{1+\sqrt{1-e^2}}{4(1-e^2)^{3/2}} de^2 + n^{5/3} \frac{(1+\sqrt{1-e^2})e^2}{4(1-e^2)} d\omega^2, \quad (16)$$

and (n, e, ω) are orthogonal coordinates, singular for circular orbits ($e = 0$).

4.3.2. Normal coordinates

4.3.2.1. Geometric preliminaries

The elliptic elements (n, e, ω) are *orthogonal coordinates* [BOL 00], which is an important geometric reduction for the metric. Further normalizations are needed to describe the geometric properties of the extremals and perform a complete analysis. In particular, since the Hamiltonian is not depending on ω , the coordinate is *cyclic* and its dual variable p_ω is a first integral of the averaged motion. As a result, if we restrict the system to the four-dimensional symplectic subspace $\{\omega = p_\omega = 0\}$, the Hamiltonian is analytic and is associated with a planar Riemannian metric defined on the restricted two-dimensional elliptic subdomain $X_0 = \{n > 0, |e| < 1\}$ by

$$ds^2 = \frac{dn^2}{9n^{1/3}} + n^{5/3} \frac{1+\sqrt{1-e^2}}{4(1-e^2)^{3/2}} de^2. \quad (17)$$

Geometrically, the condition $p_\omega = 0$ is the transversality condition for a transfer towards a circular orbit, where the angle of the pericenter is not prescribed. This is the case for the important practical problem of steering the system to the *geostationary orbit*.

The main step when computing a normal form is to reduce the corresponding metric, see [BON 06c].

Proposition 4.4. *In the appropriate domain, the planar metric is isomorphic to $ds^2 = du^2 + u^2 dv^2$ (polar form) with $u = (2/5)n^{5/6}$ and $v = (5/4)\arcsin(1-2\sqrt{1-e^2})$. In suitable coordinates, the geodesics associated with the averaged transfer towards circular orbits are straight lines.*

Theorem 4.5. *The extremal flow defined by the averaged Hamiltonian \bar{H}_r is completely integrable.*

For detailed proof, see again [BON 06c].

4.3.3. *Existence*

The two-dimensional elliptic subdomain X_0 is defined in polar coordinates by two copies of $\{u > 0, v \in]-v_c, v_c[\}$, where $c = 4/5$ and $v_c = \pi/(2c) = 5\pi/8$. Indeed, the change of variables $v = (1/c)\arcsin(1 - 2\sqrt{1-e^2})$ has a multiform inverse when e belongs to $] -1, 1[$ and the two copies have to be glued together along $e = 0$ to obtain the full elliptic subdomain. We set $X_0^- = X_0 \cap \{e > 0\}$ (respectively $X_0^+ = X_0 \cap \{e < 0\}$) and study now the contact with $e = 0$, as well as transitions from one copy to another, see figures 7(i) to 7(iii).

Proposition 4.6. *Contacts with $e = 0$ are either stationnary points or reflections from X_0^- to X_0^+ (or conversely) in flat coordinates.*

Proof. Since the averaged Hamiltonian is quadratic in the adjoint state, $e = \text{constant}$ and $p_e = 0$ are stationnary points of the system. More precisely,

$$\begin{aligned}\dot{e} &= \frac{4(1-e^2)^{3/2}}{1+\sqrt{1-e^2}} p_e, \\ \dot{p}_e &= \frac{4e\sqrt{1-e^2}(3+2\sqrt{1-e^2})}{(1+\sqrt{1-e^2})^2} p_e^2,\end{aligned}$$

and $\dot{e} \neq 0$ outside the stratum $p_e = 0$: either the contact is a stationnary point, or the sign of e changes and we go from one copy to another. In the second case, since $v = f(e^2)$ with $f = (5/4)\arcsin(1 - 2\sqrt{1-e^2})$, \dot{v} has opposite left and right limits at a time such that $e = 0$:

$$\dot{v}_+ = -\dot{v}_- = \frac{5\sqrt{2}}{4} \dot{e} \neq 0.$$

Now, since $x = u \exp(iv)$ in flat coordinates, $\dot{x} = (\dot{u} + iuv) \exp iv$ and the resulting rule

$$\dot{x}_+ - \dot{x}_- = 2i\dot{v}_+ x$$

defines a reflection at the contact with $e = 0$. □

The interplay of the multiform change of variables with the lack of geodesic convexity—that is convexity, geodesics being straight lines—of both copies of the domain is described in terms of existence by next proposition.

Proposition 4.7. *Let x_0 be in X_0^- .*

- (i) *If $v_0 \geq v'_c = \pi - v_c$, there are geodesics only towards points in X_0^- such that $v > v_0 - \pi$.*
- (ii) *If $|v_0| < v'_c$, there are geodesics towards any point in X_0^- , but only towards points in X_0^+ such that $v < \pi - 2v_c - v_0$.*
- (iii) *If $v_0 \leq -v'_c$, there are geodesics only towards points in X_0^- such that $v < \pi + v_0$, and points in X_0^+ such that $v < \pi - 2v_c - v_0$.*

The result on X_0^+ is deduced by symmetry.

Proof. Obvious, see figures 7(i) to 7(iii). In case (ii), for instance, X_0^- is starshaped with respect to x_0 , whence the geodesic accessibility of any point within the copy. \square

4.4. Optimality results and Riemannian spheres

4.4.1. Preliminaries

Consider the averaged Hamiltonian $\bar{H}_r(x, p)$ where $x = (n, e, \omega)$ and $p = (p_n, p_e, p_\omega)$ associated with the metric \bar{g} defined by (16). We parameterize geodesics by arc-length by restricting the averaged Hamiltonian to the level set $\bar{H} = 1/2$. We note $S(x_0, r)$ the Riemannian sphere with center x_0 and radius r . The *conjugate locus* $C(x_0)$ is the set of first conjugate points when we consider all the extremals starting from x_0 . The point where the extremal ceases to be minimizing is called the *cut point* and the set of cut points form the *cut locus* $L(x_0)$.

The standard results in Riemannian geometry [GAL 87] are applied to make a complete analysis. If the radius is small enough, the sphere is formed by extremities of extremal curves and we get global results by extending such curves. A cut point is either a conjugate point or a point where two minimizing geodesics with equal length are intersecting. At such points, the sphere is not smooth. As a consequence, the inspection of the extremal flow permits to decide on global optimality. The COTCOT algorithm is used to evaluate the conjugate points.

4.4.2. Geometric analysis and global optimality

Using Proposition 4.4, we get that extremal curves of the two-dimensional subsystem are globally straight lines. This allows to solve the problem of transfer towards circular orbits.

To complete the analysis, it is sufficient to analyze the extremals of the two-dimensional Riemannian metric $dv^2 + G(v)dw^2$ [BON 06d]. The covariant function $G(v)$ is related to the Gauss curvature. It governs the distribution of conjugate points according to Jacobi equation, and the conjugate locus can be computed.

4.4.3. Numerical simulations

Although explicit computations are tractable thanks to complete integrability, we can also use numerical simulations to represent Riemannian spheres and conclude about optimality. Besides, those simulations are necessary to give comparisons between the extremals of the averaged and the original Hamiltonians. The method of continuation is then fruitful to initialize the computation of the real system trajectories.

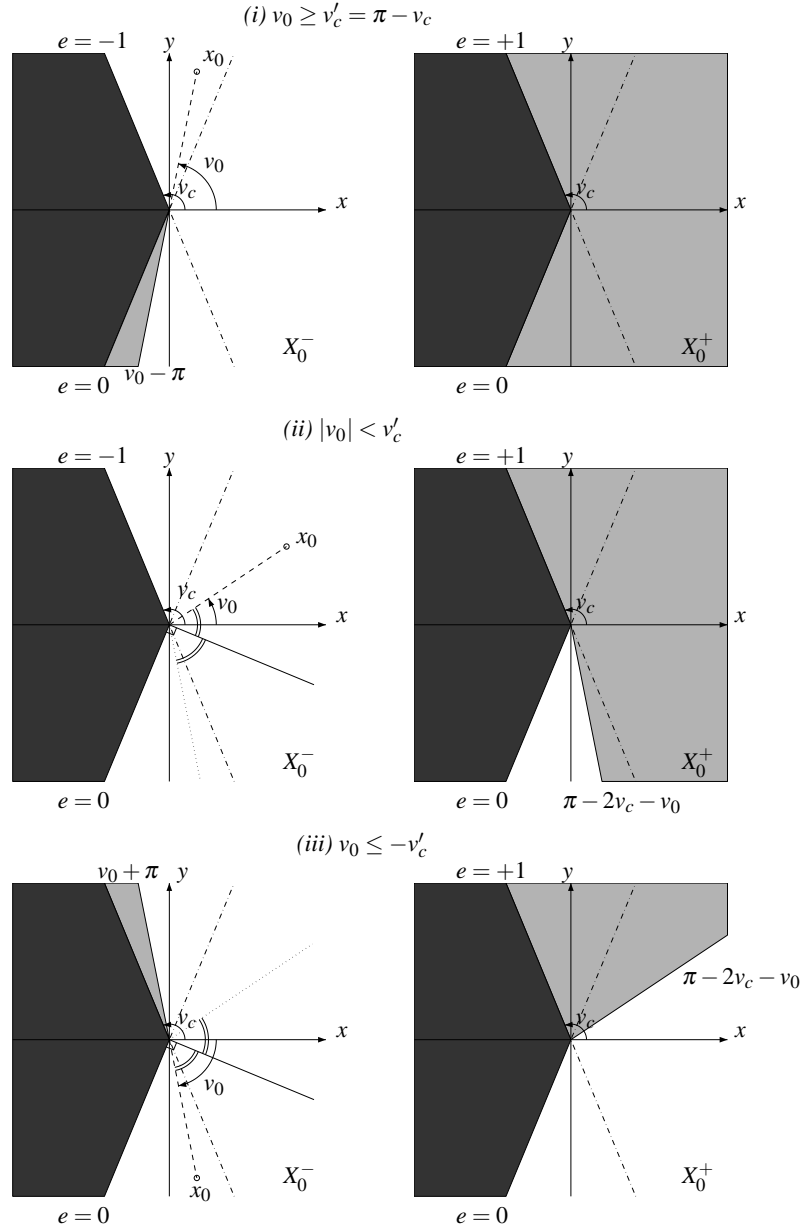


Figure 7. Domains of existence of optimal solution. Given $x_0 \in X_0^-$, i.e. with negative eccentricity, we obtain (in white) the set of points x_f in X_0^- and X_0^+ for which an optimal solution from x_0 and x_f exists. The sub-domain in X_0 where such solutions do not exist is represented in light gray. The domain in dark gray is outside the elliptic domain.

In all figures, we consider $x_0 = (e_0, n_0, \omega_0) = (0.75, 0.5, 0)$. On figure 8 we represent geodesics of the transfer to circular orbits, that is minimizing extremals such that $\omega = p_\omega = 0$. The figure 9 is a projection of the extremals in the plane (v, w) and corresponds to extremals of the metric defined in Proposition 4.4. On figure 10 we eventually compare minimizing trajectories of the averaged system with the minimizing trajectory of the real problem sharing the same boundary conditions, thus illustrating the convergence of the continuation method.

Acknowledgements

This work is supported in part by the French Space Agency (contract 02/CNES/0257/00) and done in the framework of the HYCON Network of Excellence, contract number FP6-IST-511368. Romain DUJOL is CTS (*Control Training Site*) fellow number HPMT-GH-01-00278-101.

5. References

- [All 90] ALLGOWER E., GEORG K., *Numerical continuation methods: an introduction*, Springer-Verlag, New York, 1990.
- [ARN 78] ARNOLD V. I., *Mathematical Methods of Classical Mechanics*, Springer-Verlag, New York, 1978.
- [BOL 00] BOLSINOV A. V., FOMENKO A. T., *Integrable geodesics flows on two dimensional surfaces*, Kluwer, New York, 2000.
- [BON 03] BONNARD B., CHYBA M., *Singular trajectories and their role in Control Theory*, vol. 40 of *SMAI - Mathématiques et Applications*, Springer, 2003.
- [BON 05a] BONNARD B., CAILLAU J.-B., “Advanced Topics in Control Systems Theory”, vol. 328 of *Lecture Notes in Control and Information Sciences*, chapter 1 - Introduction to Nonlinear Control, Springer-Verlag, 2005, Lecture Notes from FAP 2005.
- [BON 05b] BONNARD B., CAILLAU J.-B., DUJOL R., “Averaging and optimal control of elliptic Keplerian orbits with low propulsion”, *22nd IFIP TC7 Conference*, 2005.
- [BON 05c] BONNARD B., CAILLAU J.-B., TRÉLAT E., “Geometric optimal control of elliptic Keplerian orbits”, *Discrete and Continuous Dynamical Systems - Series B*, vol. 5, num. 4, 2005, p. 929 – 956.
- [BON 06a] BONNARD B., CAILLAU J.-B., DUJOL R., “Note sur la moyennation appliquée au transfert orbital”, report num. RT/APO/06/4, Avril 2006, ENSEEIHT-IRIT.
- [BON 06b] BONNARD B., CAILLAU J.-B., DUJOL R., “Smooth homotopies for single-input time optimal orbital transfer”, *13th IFAC Workshop on Control Applications of Optimisation*, Cachan, France, April 26-28 2006.
- [BON 06c] BONNARD B., CAILLAU J.-B., DUJOL R., “Energy minimization of single input orbit transfer by averaging and continuation”, *Bulletin des Sciences Mathématiques*, , to appear, 2006.
- [BON 06d] BONNARD B., CAILLAU J.-B., TRÉLAT E., “Second-order optimality conditions in optimal control with applications to spaceflight mechanics”, *6th AIMS Conference on*

Dynamical Systems, Differential Equations and Applications, Poitiers, France, June 25-28 2006.

- [BON 06e] BONNARD B., CAILLAU J.-B., TRÉLAT E., “Second order optimality conditions in the smooth case and applications in optimal control”, *ESAIM-COCV*, , to appear, 2006.
- [BON ed] BONNARD B., CAILLAU J.-B., “Riemannian metric of the averaged energy minimization problem in orbital transfer with low thrust”, *Ann. I. H. Poincaré*, submitted.
- [Cai 00] CAILLAU J.-B., “Contribution à l’étude du contrôle en temps minimal des transferts orbitaux”, PhD thesis, Institut National Polytechnique de Toulouse, Novembre 2000.
- [CAI 03] CAILLAU J.-B., GERGAUD J., NOAILLES J., “3D Geosynchronous Transfer of a Satellite: Continuation on the Thrust”, *Journal of Optimization Theory and Applications*, vol. 118, num. 3, 2003, p. 327 – 350.
- [CHA 87] CHAPLAIS F., “Averaging and deterministic optimal control”, *SIAM Journal Control and Optimization*, vol. 25, num. 3, 1987, p. 767 – 780.
- [GAL 87] GALLOT S., HULIN D., LAFONTAINE J., *Riemannian geometry*, Springer-Verlag, Berlin, 1987.
- [GEF 97] GEFFROY S., “Généralisation des techniques de moyennation en contrôle optimal, application aux problèmes de rendez-vous orbitaux à poussée faible”, PhD thesis, Institut National Polytechnique de Toulouse, France, Octobre 1997.
- [Ger ar] GERGAUD J., HABERKORN T., “Homotopy Method for minimum consumption orbit transfer problem”, *ESAIM-COCV*, , 2006, to appear.
- [SAR 82] SARYCHEV A. V., “The index of second variation of a control system”, *Math USSR Sbornik*, vol. 41, 1982, p. 338–401.

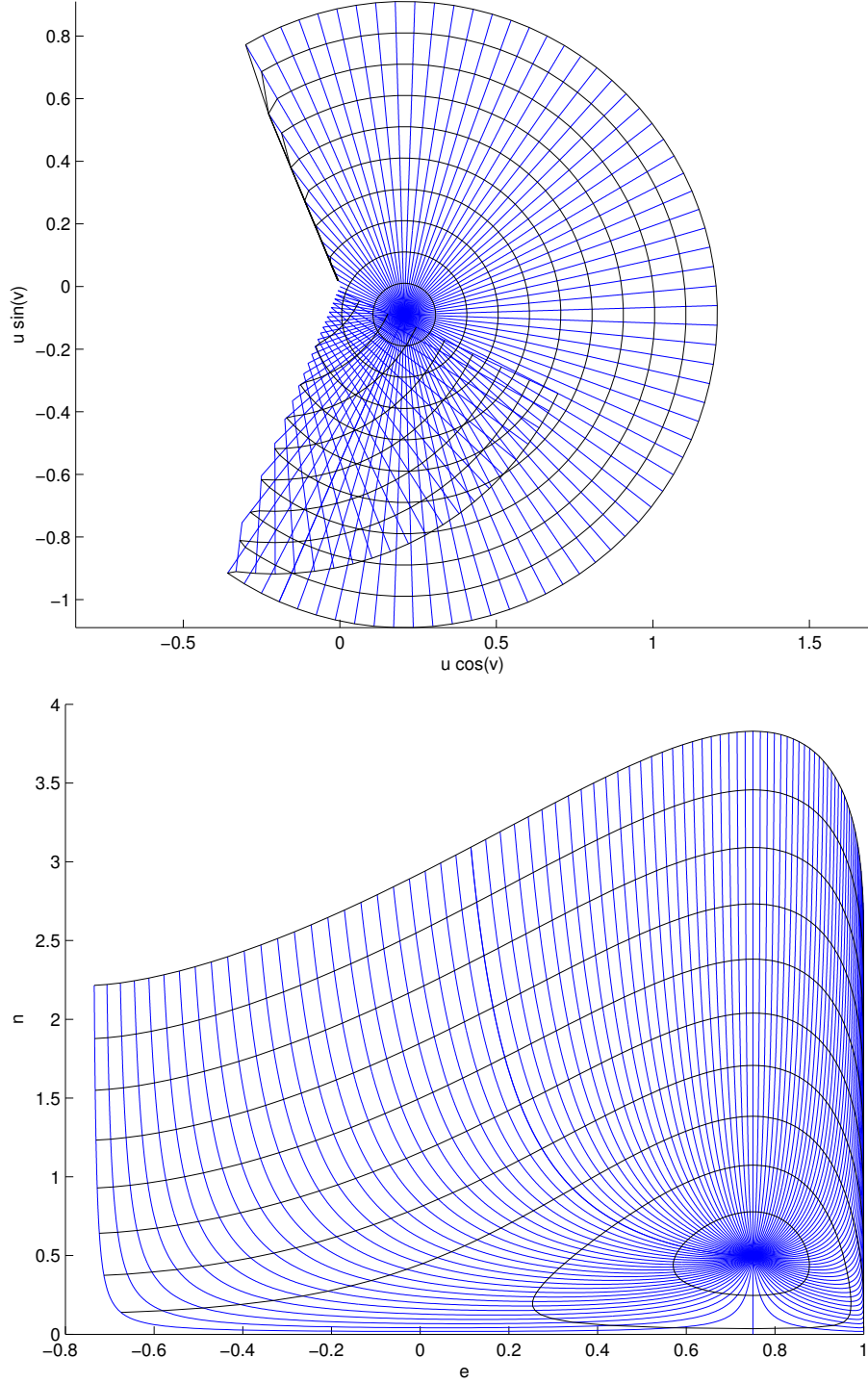


Figure 8. Geodesics of the transfer towards circular orbits up to length 1, and spheres for radii between $1e - 1$ and 1. On the first graph, flat coordinates are used and the multiform character of the change of variables from Proposition 4.4 is illustrated by the reflexion phenomenon on $v = -5\pi/8$. As shown on the second graph in coordinates (e, n) , there is no self-intersection in the two-dimensional elliptic subdomain, and the singularity $e = 0$ is smoothly crossed by geodesics.

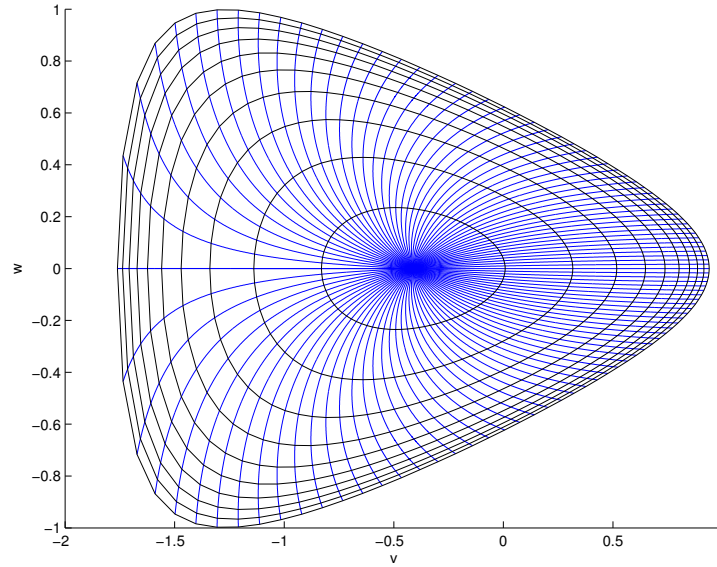


Figure 9. Geodesics up to length 1 of the transfer projected on the (v, w) -space, and associated spheres for radii between $1e - 1$ and 1.

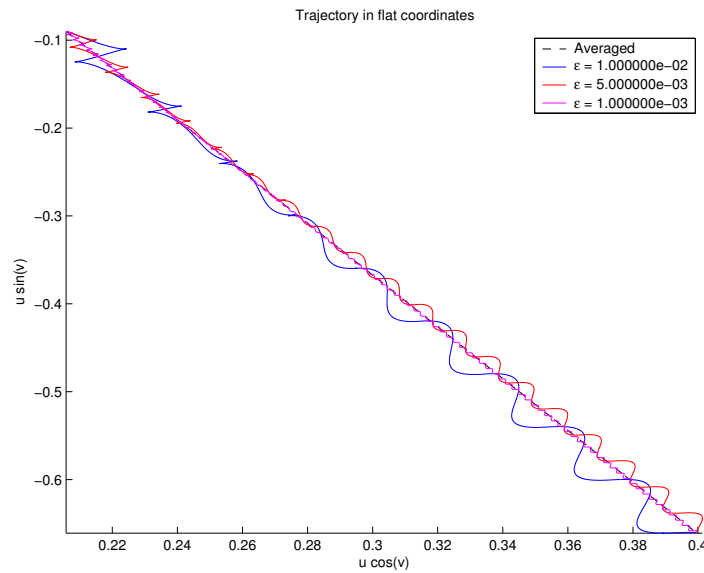


Figure 10. Computation by continuation of the non-averaged solution. The averaged trajectories are clearly nice approximations of the optimal one of the original system. Hence, convergence of the underlying shooting method to compute the non-averaged minimizing trajectory is easily obtained.

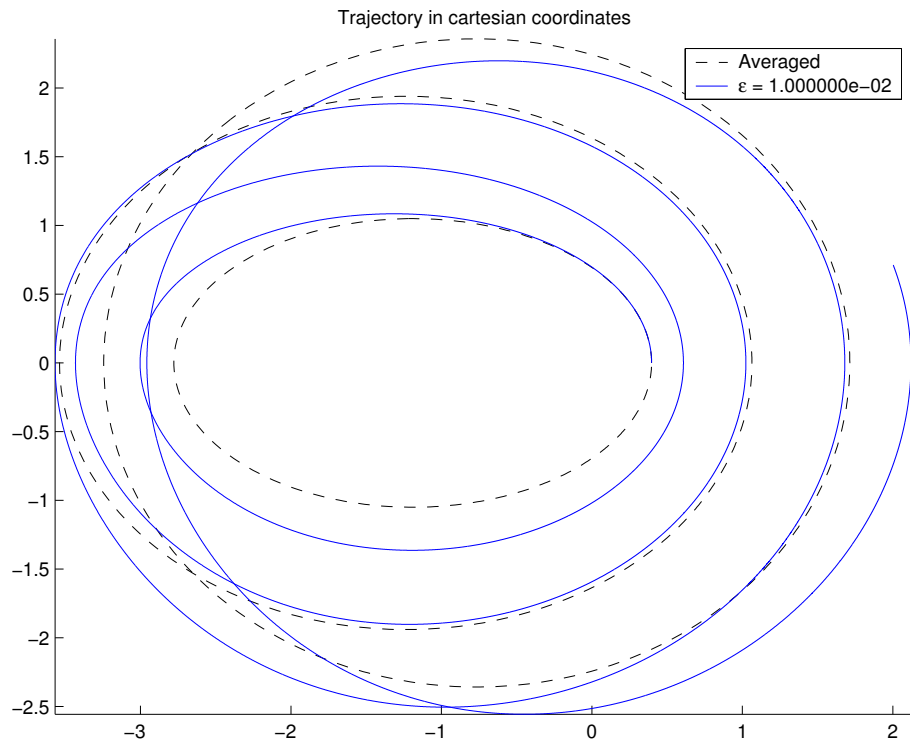


Figure 11. Trajectory of a non-averaged solution for $\varepsilon = 1e - 2$ with $(e(0), n(0)) = (0.75, 0.5)$ $(e(t_f), n(t_f)) = (0.05, 0.3)$. Dashed ellipses are averaged ellipses and provide good approximation of the motion.